Fabrication and Evaluation of Luliconazole Loaded Leciplex against Candidiasis

Gaurirani Anil Telang [a], Ashish Ashok Monde [a], Kiran Sadashiv Ashtekar [a] and Uddhav Suresh Bagul [a*]

[a] Department of Pharmaceutics, STES's Sinhgad Institute of Pharmacy (Affiliated to Savitribai Phule Pune University), Narhe, Pune 411041, Maharashtra, India.

Authors' contributions

This work was carried out in collaboration among all authors. All authors read and approved the final manuscript.

Original Research Article

ABSTRACT

Background: Fungal infections pose a significant public health concern due to the extended duration of treatment needed and the frequent reoccurrence of the disease.
Objectives: This study was aimed to enhance the permeability of luliconazole with sustain release for prolonged period for the effective treatment of fungal infection by incorporating it into lipid based nanocarrier system.
Methods: Luliconazole loaded leciplex were prepared by one step fabrication method using phospholipid, Dimethyldidodecyl ammonium bromide and transcutol P. The prepared leciplex were optimized by using Box Behnken statistical design. Furthermore, luliconazole loaded leciplex were incorporated into carbopol gel system and evaluated for various parameters.

_____

*Corresponding author: E-mail: usbagul2016@gmail.com;

Results: The luliconazole loaded leciplex showed high entrapment efficiency (98.8% ± 1.2) and size were recorded around 428.11 nm with a polydispersity index value of 0.35 ± 0.12, along with zeta potential of +26.30 mV. The Transmission Electron Microscopy studies revealed the spherical morphology of the leciplex. The developed leciplex gel was evaluated for its pH, viscosity, spreadability, hardness and adhesiveness. Furthermore, *in vitro* and *ex vivo* release kinetics demonstrated the sustained drug release pattern. Moreover, histopathology studies conducted on the rat skin revealed that the prepared formulation was non - irritant and non – toxic. The antifungal assay of developed formulations (containing only 0.3 % w/v luliconazole) showed significantly greater antifungal activity against *Candida albicans* as compared to marketed formulation (containing 1 % w/v luliconazole).

Conclusion: By taking all the results in to account it can be concluded that luliconazole loaded leciplex formulation is simple to prepare and showed excellent activity in against *Candida albicans.*

ABBREVIATIONS

BBD   *: Box-Behnken Design*
DDAB   *:Dimethyldidodecylammonium Bromide*
DoE   *: Design of Experiments*
DSC   *: Differential Scanning Calorimetry*
EE   *: Entrapment Efficiency*
LCZ   *: Luliconazole*
LP.   *: Leciplex*
LCZ – LP   *: Luliconazole loaded Leciplex*
LCZ – LPG   *: Luliconazole Leciplex Loaded Gel*
NM   *: Nanometre*
PDI   *: Polydispersity Index*
PS   *: Particle Size*
RPM   *: Rotation Per Minute*
SAED   *: Selected Area Electron Diffraction*
TEM   *: Transmission Electron Microscopy*
ZOI   *: Zone of Inhibition*

1. INTRODUCTION

In recent years, nanotechnology has made impressive strides, particularly in the development of innovative nanoparticle-based drug delivery systems. This field offers promising opportunities for research and has become an attractive area of study. The term "nano" originates from the Greek word for 'dwarf' [1]. Nanotechnology involves modifying and rearranging materials that have atomic and molecular dimensions that fall within the range of 1 to 100 nanometres [2]. Scientists aim to create drug delivery systems with effective drug loading, longer storage life, and low toxicity [3,4]. It is well known that nanoparticles are highly efficient in facilitating controlled and precise drug delivery [5].

Fungal infections pose a significant public health concern due to the extended duration of treatment needed and the frequent reoccurrence of the disease [6]. Every year, there are over 150 million cases of severe fungal infections globally, resulting in approximately 1.7 million deaths annually [7]. Among the most frequent types of fungal infections are superficial mycoses, which affect the exterior layers of the skin, hair, and nails [8].

For many years, azole compounds have been utilized as a treatment for fungal infections. One such azole antifungal agent is luliconazole, which was developed by Nihon Nohyaku Co., Ltd. in 2005 and received approval from the Food and Drug Administration (FDA) in 2013 [9]. LCZ, also referred to as NND-502, belongs to the imidazole class of antifungal drugs. Its chemical structure is unique as it incorporates the imidazole moiety into the ketene dithioacetate structure [10]. It is structurally related to lanoconazole, with a 2,4-dichlorophenyl group attached to the ketene dithioacetal structure [11]. The drug has demonstrated broad-spectrum activity against

various fungal pathogens. LCZ functions through a mechanism of action similar to other imidazole-class drugs. Ergosterol, a crucial component of the fungal membrane, plays a vital role in the proper functioning of membrane-bound enzymes [9].

Liposomes are vesicular systems composed of phospholipids that have been extensively studied for delivering various drugs to the skin. They have the ability to encapsulate a wide range of drugs, including those that are hydrophilic or hydrophobic, thereby improving their delivery through the skin [12]. Leciplex (LP) is a platform technology known for its exceptional stability due to charge interactions. It is prepared using a simple one-step fabrication process. LP, a positively charged phospholipid-based vesicular system, primarily consists of phospholipids, a cationic surfactant, and a biocompatible solvent [13].

A hydrogel is a three-dimensional structure composed of hydrophilic polymers that can retain large amounts of water. They create a moist environment that can aid in drug solubility and release [14]. Hydrogels are classified based on various characteristics such as the type and source of polymers used, crosslinking technique, sensitivity to stimuli, and ionic charge [15]. Carbomers are a type of polymer used to make carbopol. Carbomer polymers are cross-linked and form a microgel structure, making them ideal for use as a drug delivery system in dermatology [16].

This research describes a formulation of LCZ-LP in a carbopol-based hydrogel for enhanced efficacy in fungal infection therapy. First and foremost, we optimized the LP by taking into account numerous aspects. To boost its permeability, LCZ was transformed into a LP system. The LP were then incorporated into a carbopol-based hydrogel. Finally, the *in vitro, ex vivo* release profile and antifungal efficacy of LP and hydrogel were determined.

2. MATERIALS AND METHODS

2.1 Materials

Luliconazole was provided as a free sample by Akhil Healthcare (Vadodara, Gujarat). Lipoid S-100 was provided as a free sample by Lipoid GmBH (Germany). Transcutol P was obtained from Gattefosse India Pvt. Ltd. Dimethyldidodecylammonium bromide (DDAB) was purchased from Tokyo Chemical Industry

Co., Ltd. (Japan). The carbopol 974 P was obtained from Lubrizol India Private Limited, (Mumbai, India). The dialysis membrane (Mol. Weight cut off 12000 – 14000) was obtained from, Hi-Media Laboratories (Mumbai, India). The culture of *Candida albicans* was obtained from National Centre for Microbial Resource, (Pune, India). The sabouraud dextrose agar and nutrient agar were obtained from Research-lab Fine Chem Industries, (Mumbai, India). All the remaining ingredients used were of analytical grade.

2.2 Preparation of Luliconazole Loaded Leciplex (LCZ - LP)

Lecithin-based Cationic Nanoparticles were prepared by simple one step fabrication process as employed in the previously reported work (Date et al., 2011). Briefly, soybean lecithin (Lipoid S 100) at concentration of 186 mg and DDAB at the 111 mg concentration weighed precisely and transfer into a bottle containing 0.5 ml of transcutol – P. The phospholipids and DDAB were dissolved by heating the bottle at a constant temperature of 70 ℃ in water bath, after that LCZ (30mg) was added to lipid phase and heating was continued until the formation of clear homogenous solution. Thereafter, 9.5 ml of double distilled water maintained at 70 ℃ was added at once to lipid phase with continues mixing at 1300 rpm till homogenous nano dispersion was formed.

2.3 Optimization of LCZ – LP by Box-Behnken Statistical Model

The LeciPlex formulations were optimised using a Box-Behnken statistical design (Design Expert®, version 13.0.1; State Ease Inc., USA). Quality by Design was utilised to optimise the created LP formulations based on the experimental data acquired thus far [17,18]. The impact of formulation variables such as Phospholipid (A), Cationic Surfactant (B), and Drug (C) ratio on dependent variables such as Entrapment efficiency (Y1), Particle size (Y2), and PDI (Y3) were studied using this statistical design. For optimisation of the LP system, the statistical design generated multiple theoretical runs consisting of three independent variables and their low (-1), medium (0), and high (+1) levels (Table 1). The Eq. (1) illustrated the software-generated quadratic model consisting of three-factor three-level designs:

$$Y = b_0 + b_1A + b_2B + b_3C + b_{12}AB + b_{13}AC + b_{23}BC + b_{11}A^2 + b_{22}B^2 + b_{33}C \qquad (1)$$

Where Y is the measured response for each component level combination, b0 is the intercept, b1 through b3 represent the regression coefficients, and A, B, and C are independent variable coded levels [19].

2.4 Evaluation of LCZ – LP

2.4.1 Particle size and polydispersity index

The particle size and size distribution of LCZ - LP suspended in distilled water were measured at room temperature using photon correlation spectroscopy on a Nanophox Sympatech, Germany. The particle size was determined using the dynamic light scattering principle based on the time variation of scattered light from suspended particles under Brownian motion [20].

The Poly Dispersity Index (PDI) is determined by Eq. 2 equation and indicates particle distribution uniformity in the formulation.

$$PDI = (X90-X50) / X10 \qquad (2)$$

X_{90} indicates that 10% of particles are larger than the particle size at X_{90}. Conversely, X_{10} indicates that 90% of particles are smaller than the particle size at X_{10}. X_{50} denotes the average particle size.

2.4.2 Entrapment efficiency

The free quantity of LCZ was measured to determine the entrapment efficiency in LCZ - LP, which indicates the percentage of active components in the formulation (Eq. 3). To achieve this, 1 mL LCZ - LP dispersion was centrifuged at 14000 rpm for 30 minutes in an Eppendorf Mini-centrifuge. Electrolytes like NaCl were added to assist in the separation of nanoparticles. After sufficient dilution, the resulting supernatant was examined at a wavelength of 295 nm using a validated UV-spectrophotometric technique to determine the concentration of unencapsulated LCZ [21,22].

$$\%EE=(T-C) / T \times 100 \qquad (3)$$

Where, T is the total amount of LCZ used in the formulation and C is the amount of LCZ in the supernatant.

Table 1. BBD represents independent variables with their levels and measured responses from experimental runs

Run	Independent variables with their levels			Responses		
	A	B	C	Y1 (%)	Y2 (nm)	Y3
1	0	0	0	98.8	428.11	0.38
2	0	0	0	98.8	428.11	0.38
3	0	-1	1	97.6	456.68	0.31
4	1	0	-1	94.2	462.87	0.28
5	1	0	1	96.3	442.68	0.28
6	1	1	0	95.4	507	0.27
7	-1	0	-1	95.2	495.29	0.36
8	0	0	0	98.8	428.11	0.38
9	0	1	-1	94.1	518	0.31
10	0	-1	-1	96	480.03	0.28
11	-1	-1	0	94	429.01	0.28
12	0	-1	0	96.51	463.69	0.28
13	-1	0	1	97	480	0.34
14	0	0	0	98.8	428.11	0.38
15	0	0	0	98.8	428.11	0.38
16	0	-1	1	94.7	402.34	0.28
17	0	1	0	98	467.65	0.29

Independent variables	Levels		
	Low (-1)	Medium (0)	High (+1)
A= Phospholipid (mg)	157	188.5	220
B= Surfactant (mg)	92.5	110.7	129
C= Drug (mg)	25	30	35

Dependent variables
Y1= Entrapment efficiency   Y2= Particle size   Y3= Poly Dispersity Index

2.4.3 Zeta potential

The surface properties of nanoparticles are crucial for targeted drug delivery. A proper zeta potential can enhance drug release and dosage form stability at specific sites [23]. Zeta potential measurement using Delsa Nano C (USA) can optimize drug release and dosage form stability [24].

2.4.4 Differential Scanning Calorimetry (DSC)

DSC analysis of the pure drug, blank leciplex and optimized batch were carried out by using Perkin Elmer 4000 instrument having PYRIS Version-11.1.0.0488 software, 2009. DSC was used to determine whether the drug was fully entrapped in the lipids or not [25].

2.4.5 TEM and SAED images

The internal structure of the LP was determined using transmission electron microscopy (TEM). Transmission electron microscopy (TEM; FEI Tecnai T 20, USA) was used to examine the morphology of the created LCZ LP. In order to ensure even blending, the sample used for analysis was thinned out with water by a factor of 10. SAED is used with S/TEM to analyze a sample's crystallinity, lattice parameters, crystal structure, and orientation by examining the electron diffraction pattern produced by the interaction of the electron beam with the sample atoms. The technique can be used to calculate the d-spacing of crystal planes in both monocrystalline and polycrystalline structures [26].

2.5 Incorporation of LCZ – LP into Hydrogel (LCZ – LPG)

Carbopol 974p was used to create a 1% gel through the cold technique. A certain amount of Carbopol 974p was weighed and combined with a desired amount of refrigerated water. The mixture was agitated with a magnetic stirrer before TEA (Triethyl amine) was added to adjust the pH to 5.5. After refrigeration overnight, an optimised batch of LCZ - LP (equivalent to 1% LCZ) was added and mixed simultaneously until a homogenous mixture was obtained [27].

2.5.1 Evaluation LCZ – LPG

2.5.1.1 Clarity, appearance and pH

The clarity of the developed formulation before and after gelation was evaluated using white and black background to determine the appearance and clarity of the formulation. Additionally, the pH of the formulation was measured using a calibrated digital pH meter (EQ-610, Equip-Tronics, Mumbai, India). All experiments were carried out in triplicate, and the average reading was recorded [28].

2.5.2 Rheological studies

The viscosity of the prepared gel was determined using a Brookfield viscometer (Brookfield DV-II+ PRO, Mumbai, India) and spindle number of 94. The Brookfield viscometer's sample holder was filled with gel sample, and the spindle was put into the sample holder. The spindle was revolved at 100 revolutions per minute. All rheological investigations were carried out at room temperature [29].

2.5.3 Determination of spreadability

A pre-marked circle of 1 cm diameter on a glass slide was filled with 0.1g of gel, which was then covered with a second glass slide. For 5 minutes, a weight of 200 g was permitted to rest on the upper glass slide. The pressure-induced increase in diameter was observed [30].

2.5.4 Texture analysis

The formulation texture qualities are critical components in the optimisation of topical formulations. These features influence the formulation's applicability at the administration location as well as the therapeutic effect. The texture qualities of hydrogel were determined using the Brookfield CT3 texture analyser [31].

2.5.5 In-vitro drug release study

An *in-vitro* release study was conducted using a vertical Franz diffusion cell with a surface area of 2.08 cm^2 and a reservoir capacity of 20 ml. A dialysis membrane was inserted between the two sides of the cell. On the donor side, a pre-determined amount of LCZ – LPG was kept, while the receptor compartment was filled with phosphate buffer solution (pH 5.5) and swirled continuously with a magnetic stirrer at 37±0.5°C. To maintain the sink condition, 1 ml of the sample was removed from the receptor compartment at regular intervals and replaced with an equivalent volume of fresh receptor fluid. The aliquots were diluted with receptor media before being analyzed using a UV spectrophotometer. The experiment was

repeated three times, and the average data was recorded and reported. The release kinetics of LCZ – LPG were compared to marketed luliconazole cream (1% w/w) and LCZ – LP [32].

2.5.6 Ex-vivo permeation study

The *ex-vivo* diffusion experiment was carried out on rat skin. After removing the subcutaneous fat via blunt dissection, the epidermal layer was exfoliated to expose the dermal layer the skin. The skin was washed with the cold phosphate buffer in order to remove the proteins matter and the prepared skin was soaked in the PBS for the hydration. The skin was placed on the Franz diffusion cell, with the epidermal side facing the donor compartment and the dermal side in contact with the receptor solution. A specific amount of LCZ – LPG was applied to the donor side. The receptor compartment was filled with phosphate buffer solution (pH 5.5) and swirled continuously with a magnetic stirrer at $37 \pm 0.5°C$.1 ml aliquots of samples were accurately withdrawn at predetermined time intervals (0.5, 1,2,3,4,5,6,7 and 8h) using sink condition. The collected samples were diluted with phosphate buffer. The absorbance was measured using a UV visible spectrophotometer at 295 nm. The kinetics of LCZ – LPG release were compared to that of commercial luliconazole cream [33].

2.5.7 Histopathology study

Histopathology studies were carried out after exposure (8 h) of formulations to check the irritation potential by using rat skin. Prior to the study, the experimental protocol (SIOP/IAEC/2022/02/10) was approved by the Institutional Animal Ethical Committee. The samples were divided as untreated skin (negative control), treated (LCZ – LPG formulation) and skin exposed to potassium hydroxide 10 % w/v (positive control). All the skin sections were treated with 10 % v/v formalin solution followed by dehydration with alcohol. The haematoxylin and eosin were employed for staining and observed under the microscope (Motic B1 – 211 A, Asia Pacific) [34].

2.5.8 Antifungal assay

An antifungal experiment was conducted using the agar cup diffusion method to evaluate the activity of the formulations against *Candida albicans*. Before the antifungal study, all the necessary apparatus and prepared broth were autoclaved at 15 psi, 121°C for 20 minutes. The fungi were cultured on sabouraud dextrose agar,

and *Candida albicans* strains were distributed on a solidified agar plate prepared with the same media under sterile conditions (Khare et al., 2022) and wells were prepared using sterile stainless still cork borer. The samples (50µl) were pipetted into wells under sterile conditions. Petri plates were marked and incubated at room temperature for 48 hours. After 48 hours, the zone of inhibition (mm) developed on the plates was measured using digital vernier calliper (MGW precision tools), and their average of three readings was taken. The inhibition zone of LCZ – LPG was compared with LCZ – LP and marketed luliconazole cream [35].

3. RESULTS AND DISCUSSION

3.1 Optimization of LCZ - LP by Box-Behnken Design

LP is a liposomal structure with unique self-assembled cationic characteristics based on phospholipids. Particle size and entrapment efficiency affect stability and effectiveness. The drug, surfactant, and phospholipid concentrations impact entrapment efficiency, particle size, and PDI. A Box-Behnken statistical design was used to assess the effects of independent variables like the molar ratio of phospholipid, surfactant, and drug on dependent variables like entrapment efficiency, particle size, and PDI with the use of seventeen experimental batches. The optimized LCZ – LP formulation was consist of LCZ (30 mg), Phospholipid (174 mg), DDAB (92.5 mg), Transcutol P (0.5 ml) and distilled water (9.5 ml). According to the experimental results, entrapment efficiency, particle size, PDI and zeta potential of the optimized batch varied from 98.8% ± 1.2, 428.11 nm, 0.35 ± 0.12 and 26.30 mV respectively.

3.1.1 Effect of independent factors on entrapment efficiency

Different batches of the formulation exhibited entrapment efficiencies ranging from 94.0% to 98.8% as shown in Table 1. The model's F-value of 8.52 indicates its significance ($p<0.0001$). The insignificant lack of fit F-value (0.2078) and the quadratic sequential *p*-value of 0.0050 demonstrate the model's importance. The predicted and modified R^2 values of the entrapment efficiency show a reasonable degree of agreement. Lastly, the precision of 9.1308 suggests that the model's applicability to design space exploration.

$$Y = 98.85 + 0.29A + 0.065B + 0.45C + 0.747AB - 0.39AC - 0.302BC - 0.375A2 - 0.377B2 - 0.05C2 \quad (4)$$
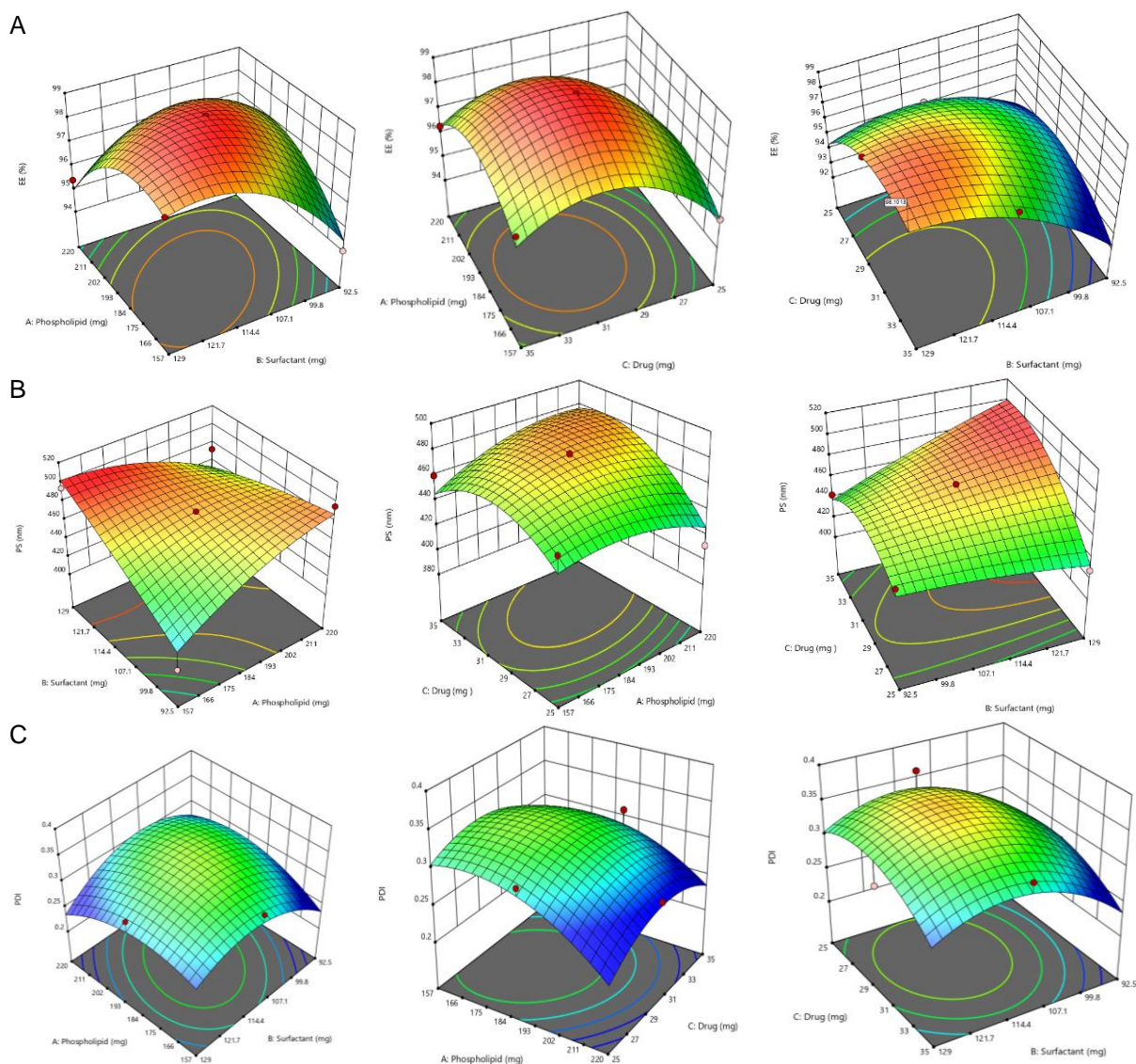
A

B

C

Fig. 1. Three-dimensional surface plots demonstrate the effect of an independent variables on (A) particle size, (B) entrapment efficiency, and (C) PDI

The positive coefficient of 'A' indicates that the entrapment efficiency increases as the amount of phospholipid increases, up to a certain point. On the other hand, the positive coefficients of 'B' suggest that the entrapment efficiency initially increases and then decreases as the amount of surfactant increases (Eq. 4). This could be due to the excess surfactant solubilizing the phospholipid, causing the drug to leak from the LP. However, when the molar ratio remains the same and the amount of phospholipid increases, the surfactant is unable to solubilize the phospholipid, resulting in the formation of tight bilayers outside the LP. This leads to an increase in entrapment efficiency. This is consistent with a prior investigation [36] in which they formulated a

moxifloxacin hydrochloride leciplex for efficient delivery to the eye. The positive coefficient of 'C' indicates that entrapment efficiency rises as the drug concentration increases. The 3-dimensional surface plot (Fig. 1A) demonstrates the impact of variations in independent variables on entrapment. The quadratic model exhibits the highest level of efficiency.

3.1.2 Effect of independent factor of particle size

Different batches of the formulation exhibited particle size ranging from 402 to 518 nm as shown in Table 1. The model's F-value of 4.61 indicates its significance (p<0.0001). The

insignificant lack of fit F-value (604.27) and the quadratic sequential *p*-value of 0.0050 demonstrate the model's importance. The predicted and modified R^2 values of the particle size show a reasonable degree of agreement. Lastly, the precision of 6.468 suggests that the model's applicability to design space exploration.

$$Y= 428+4.30A+11.45B+13.665C-28.46AB+ 11.42AC+19.84BC-10.84A2 -2.90B2 - 21.88C2 \quad (5)$$

The quadratic model is the most suitable for representing the data on particle size, as depicted in the 3D surface plot (Fig. 1B). The positive coefficient of 'A' suggests that when the concentration of phospholipid declines, the particle size also lowers. This could be attributed to the production of smaller vesicles resulting from the reduced lipid concentration. This finding aligns with the previous study [13], which involved the creation of vancomycin hydrochloride loaded leciplex. The positive coefficients of 'B' and 'C' indicate that the particle size decreases simultaneously with a drop in the concentration of surfactant and drug, respectively (Eq. 5).

3.1.3 Effect of the independent factor of PDI

Different batches of the formulation exhibited particle size ranging from 0.28 to 0.38 as shown in Table 1. The model's F-value of 4.05 indicates its significance (p<0.0001). The quadratic sequential p-value of 0.0394 demonstrate the model's importance. The predicted and modified R^2 values of the PDI show a reasonable degree of agreement. Lastly, the precision of 5.245 suggests that the model's applicability to design space exploration.

$$Y= 0.28-0.026A+0.027B-0.0087C +0.01AB + 0.007AC-0.025BC+0.026A2+0.33B2+0.031C2 \quad (6)$$

The positive coefficient 'B' indicates a decrease in the PDI as the surfactant decreases, the negative coefficient 'C' indicates a simultaneous decrease in the PDI of the leciplexes with an increase in the concentration of phospholipid and a decrease in the concentration of surfactant, and the negative coefficient 'A' indicates that there would be a decrease in PDI with the decrease in the phospholipid (Eq. 6). The 3-dimensional surface plot (Fig. 1C) shows how the independent variable changes affect entrapment, and it can be inferred that the quadratic model provides the best fit for PDI.

3.2 Evaluation and Characterization of LCZ – LP
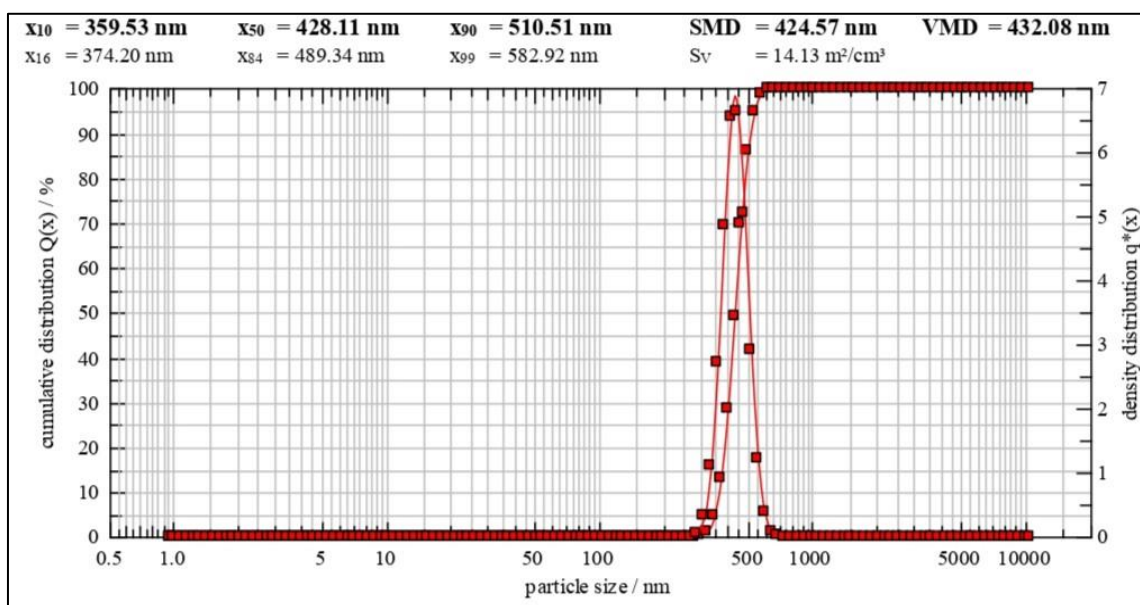
3.2.1 Particle size, PDI, % EE and zeta potential

The LCZ – LP that was created showed excellent particle size and PDI. The particle size of the LP was found to be 428.11nm (Fig. 2A) and PDI was found to be 0.35 ± 0.12. The LCZ – LP showed an encapsulation efficiency of 98.8 ± 1.2 %, showing strong interaction of LCZ with the LP. Zeta potential was found to be positive for LCZ – LP due to double chain cationic surfactant (DDAB) and, hence indicating good colloidal stability. The optimized batch showed highest zeta potential value (26.30 mV) as shown in Fig. 2B indicating stabilizing effect of cationic surfactant DDAB. The preferential of positive charge of this formula prefers a positive charge to enhance contact between cationic nanoparticles and negatively charged skin.
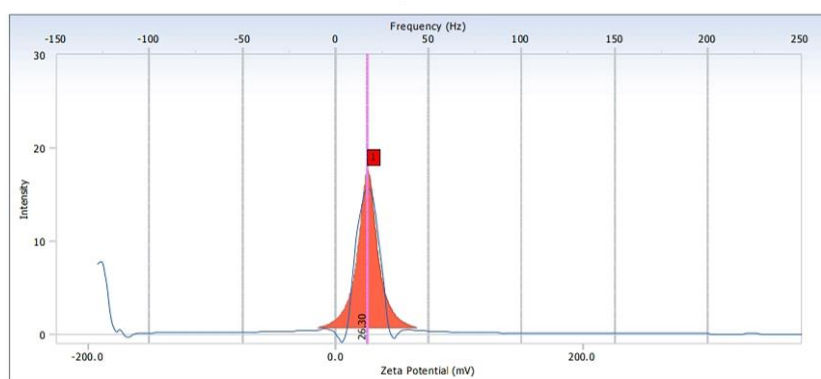
3.2.2 DSC study

The overlay of the DSC analysis of the optimized LCZ - LP batch showed the phospholipid, cationic surfactant compatibility. The A in the Fig. 3 shows the thermogram of LCZ and it shows peak at 150°C represent its melting point. The graph B and C shows the blank LP and LCZ – LP respectively. This results demonstrate the complete entrapment of luliconazole in the lipid bilayer.

3.2.3 TEM and SAED images

The dynamic light scattering approach deals with apparent size of particle along with hydrodynamic layers that surrounds the particles which leads to overestimation of the particle size[16,35]. For more accurate determination, the TEM was employed revealing micrographs of LCZ - LP with spherical, and distinct smooth surface. The particle size was consistent and appeared dark and uniformly dispersed without aggregation. (Fig. 4A). The size of particle observed under TEM was comparatively smaller than that measured by particle size analyser. Additionally, the crystallographic structure of the LCZ - LP was characterized by the SAED method. The SAED image of the optimized batch shows polycrystalline structures. It can be concluded from the Fig. 4B, that the polycrystalline structure consists of many small single crystals making it up a ring.

x_{10} = 359.53 nm	x_{50} = 428.11 nm	x_{90} = 510.51 nm	SMD = 424.57 nm	VMD = 432.08 nm
x_{16} = 374.20 nm	x_{84} = 489.34 nm	x_{99} = 582.92 nm	Sv = 14.13 m²/cm³	

A

B

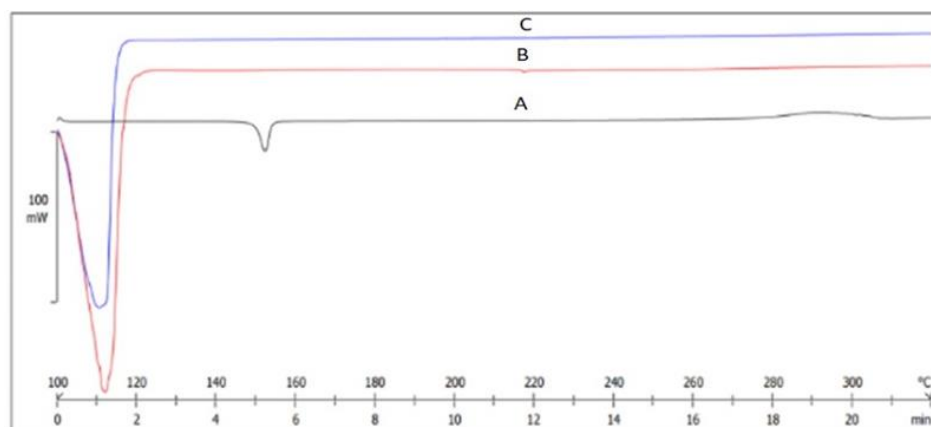**Fig. 2. Particle size (A) and zeta potential (B) of optimized batch**

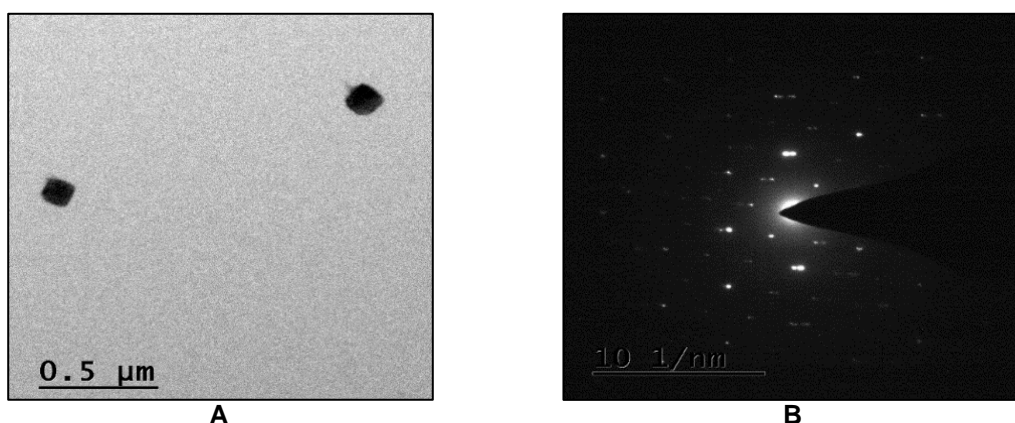**Fig. 3. DSC thermograms of pure drug (A), Blank leciplex (B) and LCZ –LP (C)**

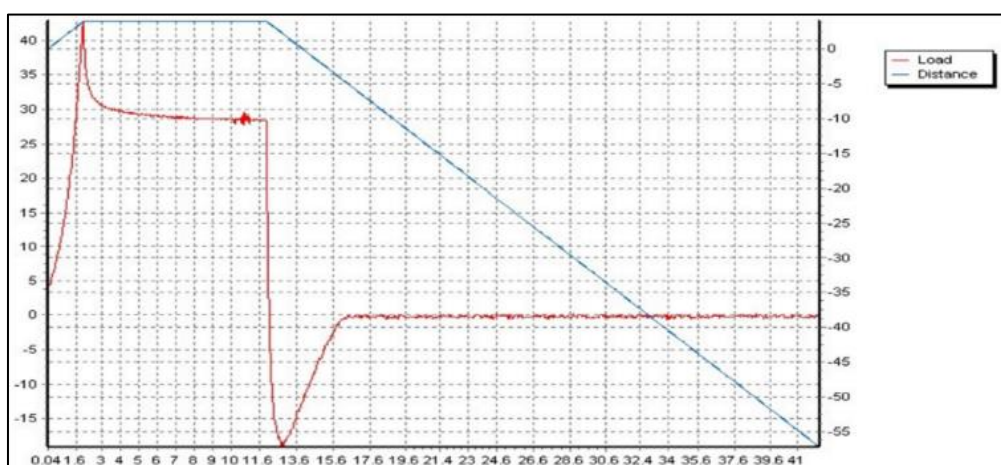**Fig. 4. TEM photomicrograph (A) and SAED (B) of optimized LCZ – LP**

Fig. 5. Texture analysis of LCZ – LPG

3.3 Evaluation of LCZ – LPG

3.3.1 Clarity, appearance and pH

It was noticed that the LCZ – LPG had a smooth and transparent appearance. To ensure the prepared LCZ – LPG was safe for use, a digital pH meter was utilized to determine its pH level. To maintain the gel's pH within the topical range, we added a small amount of triethanolamine, resulting in a pH of 5.67 ± 0.1, which closely matches the pH of the skin. It is important to adjust the pH of gel formulations to avoid skin irritation and other potential problems.

3.3.2 Viscosity

The measured viscosity of the LCZ – LPG using a Brookfield viscometer. The LCZ – LPG was placed into the sample holder of the viscometer and inserted spindle No. 91. Then the spindle was rotated at 100 rpm and found that the viscosity was 8070 ±138.95 cps, which was the desired.

3.3.3 Spreadability

It is a key factor in patient compliance. Through the use of a good spreadable formulation, the application of topical preparation became simple and consistent. To determine the spreadability of the gel, the glass plate method was utilized. The findings suggested that the gel's spreadability falls within the range of 5 to 7 cm, indicating satisfactory spreadability. In brief, after conducting the spread test for the LCZ – LPG, it was observed a value of 5.6 - 6.2 cm, which reveals the gel's robust spreadability.

3.3.4 Texture analysis

Fig. 5 summarizes the textural characteristics of the gel, such as hardness and adhesiveness. These mechanical attributes are critical for its

effective use in clinical settings. A structural examination was conducted to evaluate the adherence and hardness of the preparation. The hardness of the gel affects its flow qualities, and at lower hardness, the preparation can leak, while at higher hardness, it can be difficult to extract from the tube. After testing, it was found that the gel's composition was suitable at a hardness of 42.08 g. The gel's ability to stick to surfaces is crucial for retaining the penetrated dose around an affected area, and higher adhesiveness improves this. However, spreading the mixture over the skin's surface can be challenging. The gel's adhesiveness was found to be 0.88 mJ.

3.3.5 In-vitro analysis

The *in vitro* drug release of LCZ from LCZ – LP, LCZ – LPG and marketed formulation was carried out and compared. The Franz diffusion cell was used for this purpose, Fig. 6 depicted the percentage cumulative drug release. It is evident that release of LCZ from LP was significantly lower than marketed formulation. LCZ released more than 50% from marketed formulation in the first 4 h whereas LCZ – LP released less than 30% and LCZ – LPG released less than 20%. The marketed formulation demonstrated a cumulative drug release of 95.13 ± 2.3% at the end of 8 h. LCZ – LP suspension, on the other hand, showed a lower drug release of 85.34 ±3 % in 8 hours due to the drug being entrapped in lipids. LCZ – LPG showed a cumulative drug release of 75.85% in 8 hours. The LCZ – LPG I had a more tightly regulated drug release compared to the commercial formulation, as the LCZ – LP was integrated into

a thick and viscous structure of gel. The sustained release properties of LP could be useful in maintaining therapeutic concentration of LCZ for longer duration *in vivo.*

3.3.6 Ex-vivo permeation study

To conduct an accurate comparison of drug permeation through rat skin, an ex-vivo investigation was carried out using marketed formulation and LCZ – LPG. The amount of drug that permeated per unit of skin surface area was measured over time. Results showed that the LCZ – LPG permeated 71.23 ±3.1% as compared to 92.81 ± 2.4% from marketed formulation at the end of 8 h study (Fig. 7). Administering the drug in its thick, viscous gel form slowed down its release, resulting in a sustained release. The drug permeated from the LCZ – LPG was significantly different ($p < 0.05$) as compared to marketed formulation.

3.3.7 Histopathology study

Histopathology studies were carried out to check irritation potential of optimized LCZ – LPG formulation by using rat skin and compared with the positive control (10% w/v KOH) and negative control (PBS) for 8h exposure. The results (Fig. 8) obtained in the positive control treated skin clearly demonstrated the damage to the epidermis layer, whereas negative control and LCZ – LPG showed the presence of normal skin surface structure indicating that the prepared formulation of LCZ – LPG is non - irritant and non - toxic to the skin.
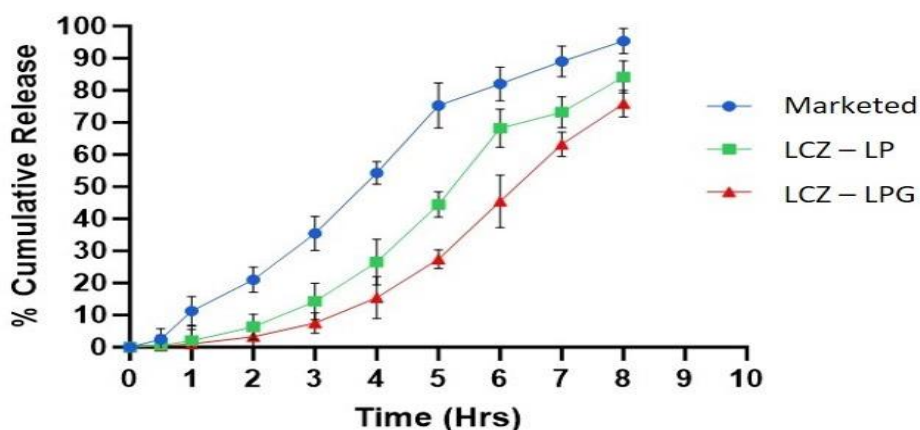

Fig. 6. *In-vitro* drug release data for LCZ – LP, LCZ – LPG and marketed formulation in phosphate buffer solution pH 5.5 (n = 3 ± SD)
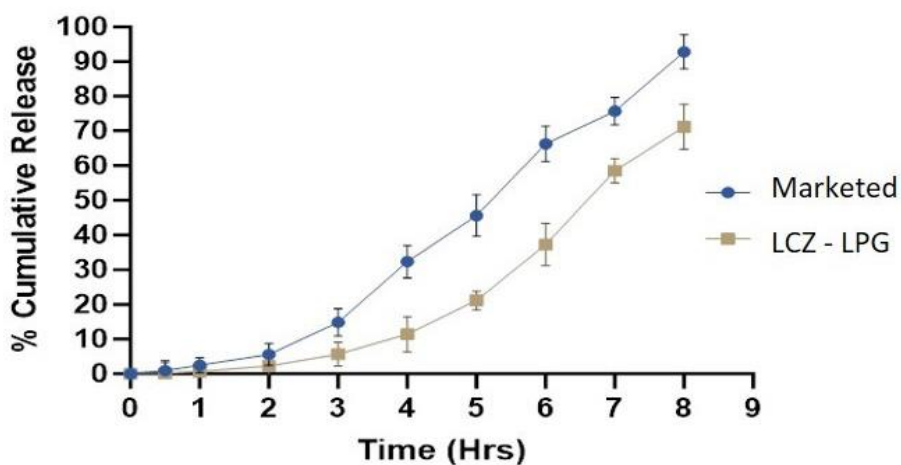
Fig. 7. *Ex-vivo* permeation profile of LCZ – LPG and marketed formulation using rat skin (n = 3 ± SD)
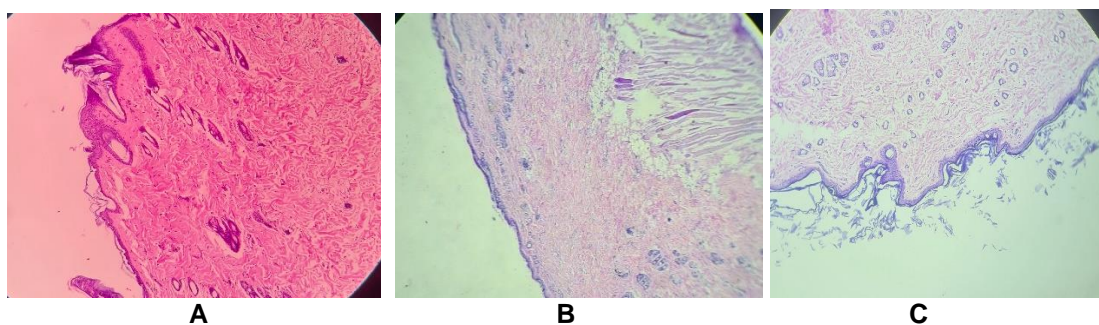

| A | B | C |

Fig. 8. Skin irritation test on rat skin (A) Positive control (10% w/v KOH) (B) Negative control (PBS) (C) LCZ – LPG

Fig. 9. Antifungal assay of marketed, LCZ – LPG and LCZ – LP against Candida albicans

3.3.8 Antifungal assay

Finally, to check the ability of LCZ – LP and LCZ – LPG formulations as a therapeutic candidate against fungal infection, antifungal study was performed on *Candida albicans* culture and compared with marketed formulation. The agar cup diffusion method was employed to establish antifungal activity. This was performed by measuring the zone of inhibition (ZOI). All the studies were performed in triplicates. Previous research have reported the use of agar cup diffusion method to evaluate the antifungal activity by measuring the ZOI in mm [37,38]. After 48 h, the antifungal observations (Table 2) depicted that incorporation of LCZ in cationic liposomes (LCZ - LP) possessed greater effect against *Candida albicans* when compared with marketed formulation. Moreover, LCZ – LPG showed greater and sustained effect due to its thick and viscous gel which limits the diffusion of drug through the gel matrix (Fig. 9).

Table 2. Zone of inhibition of different formulations in the antifungal assay

Sr. no	Formulations	Zone of Inhibition (mm)
1	Marketed	21.2 ± 1.2 mm
2	LCZ – LPG	25.3 ± 1.1 mm
3	LCZ – LP	29.1 ± 1.3 mm

4.CONCLUSION

The present study established the successful preparation and optimization of LCZ – LP using Box Behnken Design. The LCZ – LP showed high entrapment efficiency (98.8% ± 1.2) and size were recorded around 428.11 nm with a PDI value of 0.35 ± 0.12. The prepared LCZ – LP were further incorporated into carbopol gelling system. The developed LCZ – LPG was evaluated for its pH, viscocity, spreadability, hardness and adhesiveness (texture analysis). Furthermore, *in vitro* and *ex vivo* release kinetics demonstrated that the release of LCZ from LCZ – LPG was sustained release. Moreover, histopathology studies conducted on the rat skin revealed that the prepared formulation was non - irritant and non – toxic. The antifungal assay showed that LCZ – LP and LCZ – LPG have significantly greater antifungal activity as compared to marketed formulation. Hence it could be concluded that LCZ – LP and LCZ – LPG formulations are more promising in the effective treatment against *Candida albicans.*

REFERENCES

1. Chavda VP. Nanobased nano drug delivery, in: applications of targeted nano drugs and delivery systems. Elsevier. 2019;69–92.
   Available:https://doi.org/10.1016/B978-0-12-814029-1.00004-1
2. Bhushan B, Handbook of Nanotechnology, 4th ed. Springer; 2017
3. Gupta AK, Daigle D. A critical appraisal of once-daily topical luliconazole for the treatment of superficial fungal infections. Infection and Drug Resistance. 2016;1-6.
4. Alhakamy NA, Md S, Alam MS, Shaik RA, Ahmad J, Ahmad A, Kutbi HI, Noor AO, Bagalagel A, Bannan DF, Gorain B. Development, optimization, and evaluation of luliconazole nanoemulgel for the treatment of fungal infection. Journal of Chemistry. 2021;2021(1):4942659.

5. Peek LJ., Middaugh CR, Berkland C. Nanotechnology in vaccine delivery. Adv. Drug Deliv. Rev. 2008;60:915–928. Available:https://doi.org/10.1016/j.addr.2007.05.017

6. Mohammed BS, Al-Gawhari FJ. Preparation of posaconazole nanosponges for improved topical delivery system. Int. J. DRUG Deliv. Technol. 2022;12:8–14. Available:https://doi.org/10.25258/ijddt.12.1.2

7. Denning DW, Bromley MJ. How to bolster the antifungal pipeline. Science. 2015;347: 1414–1416. Available:https://doi.org/10.1126/science.aaa6097

8. Sharma B, Nonzom S. Superficial mycoses, a matter of concern: Global and Indian scenario-an updated analysis. Mycoses. 2021;64:890–908. Available:https://doi.org/10.1111/myc.13264

9. Dos Santos Porto D, Bajerski L, Donadel Malesuik M, Soldateli Paim C. A review of characteristics, properties, application of nanocarriers and analytical methods of luliconazole. Crit. Rev. Anal. Chem. 2022; 52:1930–1937. Available:https://doi.org/10.1080/10408347.2021.1926219

10. Sharma M, Mundlia J, Kumar T, Ahuja M. A novel microwave-assisted synthesis, characterization and evaluation of luliconazole-loaded solid lipid nanoparticles. Polym. Bull. 2021;78:2553–2567. Available:https://doi.org/10.1007/s00289-020-03220-5

11. Khanna D, Bharti S. Luliconazole for the treatment of fungal infections: an evidence-based review. Core Evid. 2014;113. Available:https://doi.org/10.2147/CE.S49629

12. Salama A, Badran M, Elmowafy M, Soliman GM. Spironolactone-loaded leciplexes as potential topical delivery systems for female acne: *In vitro* Appraisal and Ex Vivo Skin Permeability Studies. Pharmaceutics. 2019;12:25. Available:https://doi.org/10.3390/pharmaceutics12010025

13. Abdellatif MM, Ahmed SM, El-Nabarawi MA, Teaima M. Oral bioavailability enhancement of vancomycin hydrochloride with cationic nanocarrier (Leciplex): optimization, *In vitro*, Ex vivo, and *In vivo* Studies. Sci. Pharm. 2022;91:1.

Available:https://doi.org/10.3390/scipharm91010001

14. Narayanaswamy R, Torchilin VP. Hydrogels and their applications in targeted drug delivery. Molecules. 2019; 24:603. Available:https://doi.org/10.3390/molecules24030603

15. Bashir S, Hina M, Iqbal J, Rajpar AH, Mujtaba MA, Alghamdi NA, Wageh S, Ramesh K, Ramesh S. Fundamental concepts of hydrogels: Synthesis, Properties, and their applications. Polymers. 2020;12:2702. Available:https://doi.org/10.3390/polym12112702

16. Wang W, Narain R, Zeng H. Hydrogels, in: Polymer science and nanotechnology. Elsevier. 2020;203–244. Available:https://doi.org/10.1016/B978-0-12-816806-6.00010-8

17. Beg S. (Ed.). Design of experiments for pharmaceutical product development: Basics and Fundamental Principles. Springer Singapore, Singapore. 2021;1. Available:https://doi.org/10.1007/978-981-33-4717-5

18. Bagul US, Nazirkar MV, Mane AK, Khot SV, Tagalpallewar AA, Kokare CR. Fabrication of architectonic nanosponges for intraocular delivery of Brinzolamide: An insight into QbD driven optimization, in vitro characterization, and pharmacodynamics. International Journal of Pharmaceutics. 2023;123746. Available:https://doi.org/10.1016/j.ijpharm.2023.123746.

19. Kumbhar SA, Kokare CR, Shrivastava B, Gorain B, Choudhury H. Preparation, characterization, and optimization of asenapine maleate mucoadhesive nanoemulsion using Box-Behnken design: *In vitro* and in vivo studies for brain targeting. International Journal of Pharmaceutics. 2020;586:119499. Available:https://doi.org/10.1007/s40005-017-0318-8

20. Xu R. Progress in nanoparticles characterization: Sizing and zeta potential measurement. Particuology. 2008;6:112–115. Available:https://doi.org/10.1016/j.partic.2007.12.002

21. Date Abhijit A, Nagarsenker MS, Patere S, Dhawan V, Gude RP, Hassan PA, Aswal V, Steiniger F, Thamm J, Fahr A. Lecithin-based novel cationic nanocarriers

(Leciplex) II: Improving Therapeutic Efficacy of Quercetin on Oral Administration. Mol. Pharm. 2021;8:716–726.
Available:https://doi.org/10.1021/mp100305h

22. Date Abhijit A, Srivastava D, Nagarsenker, MS, Mulherkar R, Panicker L, Aswal V, Hassan PA, Steiniger F, Thamm J, Fahr A. Lecithin-based novel cationic nanocarriers (LeciPlex) I: fabrication, characterization and evaluation. Nanomed. 2011;6:1309–1325.
Available:https://doi.org/10.2217/nnm.11.38

23. Honary S, Zahir F. Effect of zeta potential on the properties of nano-drug delivery systems - A Review (Part 2). Trop. J. Pharm. Res. 2013;12:265–273.
Available:https://doi.org/10.4314/tjpr.v12i2.20

24. Bhattacharjee S. DLS and zeta potential – What they are and what they are not? J. Controlled Release. 2016;235:337–351.
Available:https://doi.org/10.1016/j.jconrel.2016.06.017

25. Zheng Q, Zhang Y, Montazerian M, Gulbiten O, Mauro JC, Zanotto ED, Yue Y. Understanding Glass through Differential Scanning Calorimetry. Chem. Rev. 2019;119:7848–7939.
Available:https://doi.org/10.1021/acs.chemrev.8b00510

26. Tizro P, Choi C, Khanlou N. Sample Preparation for transmission electron microscopy, in: Yong, W.H. (Ed.), Biobanking, Methods in Molecular Biology. Springer New York, New York, NY. 2019;417–424.
Available:https://doi.org/10.1007/978-1-4939-8935-5_33

27. Nurman S, Yulia R, Irmayanti Noor E, Candra Sunarti T. The optimization of gel preparations using the active compounds of Arabica Coffee Ground Nanoparticles. Sci. Pharm. 2019;87:32.
Available:https://doi.org/10.3390/scipharm87040032

28. Shankar D, Gajanan S, Suresh J, Dushyant G. Formulation and evaluation of luliconazole emulgel for topical drug delivery. Int Res J Sci Eng. 2018;3:85-9.

29. Parente ME, Ochoa Andrade A, Ares G, Russo F, Jiménez-Kairuz Á. Bioadhesive hydrogels for cosmetic applications. Int. J. Cosmet. Sci. 2015;37:511–518.
Available:https://doi.org/10.1111/ics.12227

30. Gupta A, Mishra A, Singh A, Gupta V, Bansal P. Formulation and evaluation of topical gel of diclofenac sodium using different polymers. Drug Invent. Today; 2010.

31. Hurler J, Engesland A. Poorahmary Kermany B, Škalko-Basnet N. Improved texture analysis for hydrogel characterization: Gel cohesiveness, adhesiveness, and hardness. J. Appl. Polym. Sci. 2012;125:180–188.
Available:https://doi.org/10.1002/app.35414

32. Jain A, Jain SK. *In vitro* release kinetics model fitting of liposomes: An insight. Chem. Phys. Lipids. 2016;201:28–40.
Available:https://doi.org/10.1016/j.chemphyslip.2016.10.005

33. Andréo-Filho N, Bim AVK, Kaneko TM, Kitice NA, Haridass IN, Abd E, Santos Lopes P, Thakur SS, Parekh HS, Roberts MS, Grice JE, Benson HAE, Leite-Silva VR. Development and evaluation of lipid nanoparticles containing natural botanical oil for sun protection: Characterization and *in vitro* and *in vivo* human skin permeation and toxicity. Skin Pharmacol. Physiol.2018; 31:1–9.
Available:https://doi.org/10.1159/000481691

34. Vandana G, Magar SLR, Anil S, Rani S. Evaluation of histopathological findings of skin biopsies in various skin disorders. Group. 2015;2:1-01.

35. Wani MY, Ahmad A, Kumar S, Sobral AJFN. Flucytosine analogues obtained through Biginelli reaction as efficient combinative antifungal agents. Microb. Pathog. 2017;105:57–62.
Available:https://doi.org/10.1016/j.micpath.2017.02.006

36. Albash R, M Abdellatif M, Hassan M, M Badawi N. Tailoring terpesomes and leciplex for the effective ocular conveyance of moxifloxacin hydrochloride (Comparative assessment): *in-vitro*, ex-vivo, and *in-vivo* evaluation. International Journal of Nanomedicine. 2021;5247-5263.
Available:https://doi.org/10.2147/IJN.S316326

37. Khare P, Chogale MM, Kakade P, Patravale VB. Gellan gum–based in situ gelling ophthalmic nanosuspension of posaconazole. Drug Deliv. Transl. Res. 2022;12:2920–2935.
Available:https://doi.org/10.1007/s13346-022-01155-0

38. Morsi N., Ghorab D, Refai H, Teba H. Ketoroloac tromethamine loaded nanodispersion incorporated into thermosensitive in situ gel for prolonged ocular delivery. International Journal of Pharmaceutics. 2016;506(1–2). Available:https://doi.org/10.1016/j.ijpharm. 2016.04.021.

Peer-review history:
The peer review history for this paper can be accessed here:
https://www.sdiarticle5.com/review-history/119934